CHAPTER IV
RESULTS AND DISCUSSION

4.1 Au/CeO$_2$, Au/ Fe$_2$O$_3$-CeO$_2$, and Au/Fe$_2$O$_3$ Catalysts

In this part, Au/CeO$_2$, Au/Fe$_2$O$_3$-CeO$_2$, and Au/Fe$_2$O$_3$ catalysts were prepared by a deposition-precipitation (DP) method and characterized by several techniques. The prepared catalysts were tested in the methanol steam reforming reaction. Moreover, the influences of Fe$_2$O$_3$-CeO$_2$ ratio, Au content, calcination temperature, gas pretreatment, and reaction temperature on the catalytic performance were studied in detail.

The catalytic activity tests were carried out in a vertical pyrex glass microreactor by packing with 100 mg catalyst of 80–120 mesh inside. The activity was investigated at varied temperature in the range of 250 to 450°C under atmospheric pressure. The characterization results from several techniques, including TPR, XRD, TEM, and BET of the prepared catalysts will be used to explain the catalytic activity and selectivity of the prepared catalysts in this part.

4.1.1 Effect of Temperature on the Catalytic Performance of 1%Au over Different Supports

To study effect of temperature on the catalytic performance of 1%Au over different supports, the Au/CeO$_2$, Au/ Fe$_2$O$_3$-CeO$_2$(1:8), and Au/Fe$_2$O$_3$ were prepared by deposition-precipitation technique with 1% Au content. All of them were calcined at 400°C for 3 hours. Figure 4.1 shows the methanol conversion and hydrogen selectivity in the steam reforming reaction with varying the reaction temperature from 250 to 450°C.
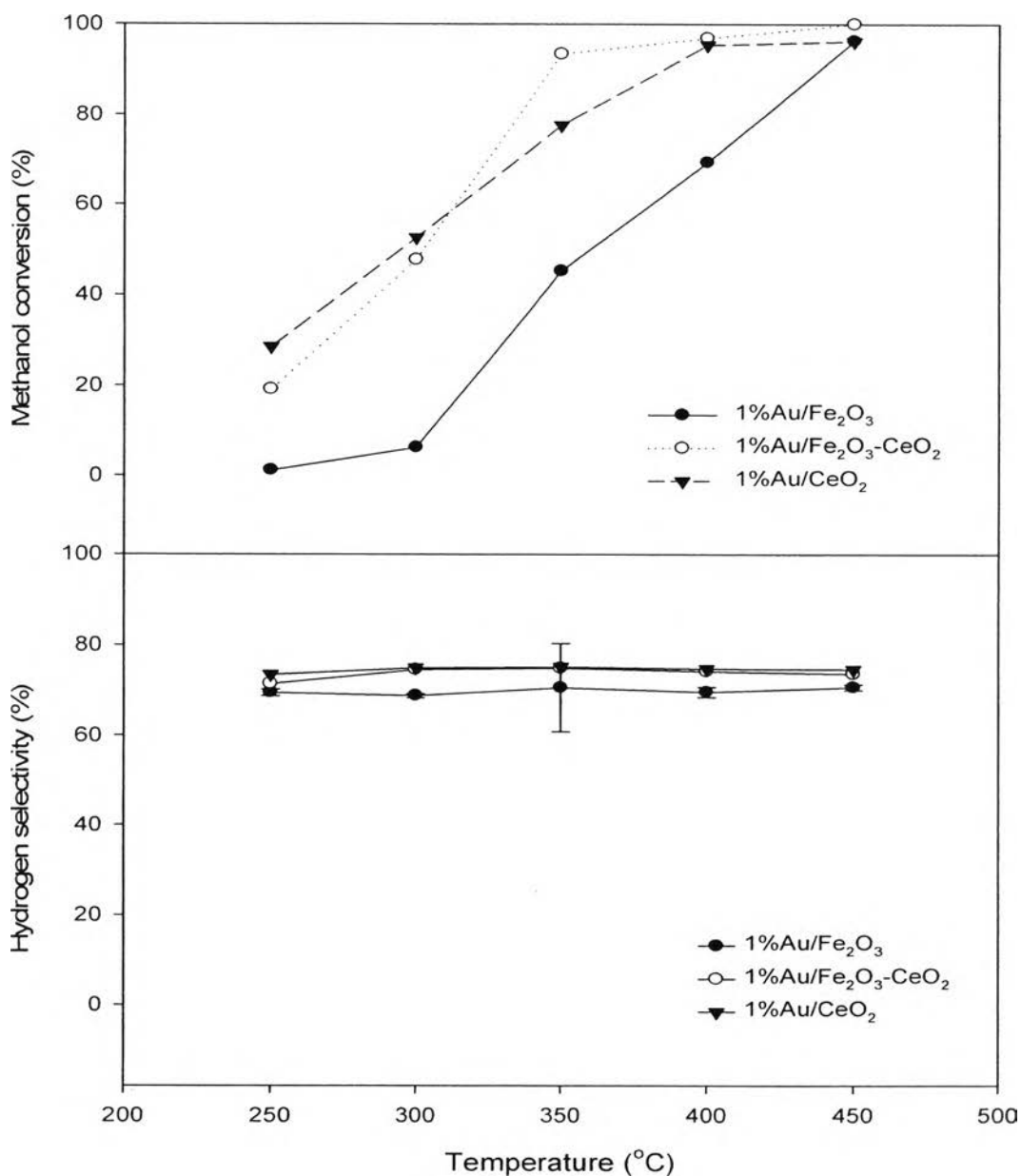
Figure 4.1 Effect of temperature on the methanol conversion and hydrogen selectivity of supported Au catalysts.

It can be seen that the 1%Au/Fe$_2$O$_3$-CeO$_2$(1:8) exhibited the highest catalytic activity at the temperature range around 300 to 400°C compared to the 1%Au/CeO$_2$ and 1%Au/Fe$_2$O$_3$. For the hydrogen selectivity, the 1%Au/Fe$_2$O$_3$-CeO$_2$(1:8) and 1%Au/CeO$_2$ gave slightly higher selectivity than the 1%Au/Fe$_2$O$_3$. It

has been reported that Fe_2O_3-CeO_2 composites enhance the catalytic activity (Kanimura *et al.*, 2003). In this work, we found that combination of both Fe_2O_3 and CeO_2 can also enhance the methanol conversion of MSR.

4.1.1.1 X-ray Diffraction (XRD)

The XRD results of 1%Au/Fe_2O_3, 1%Au/Fe_2O_3-CeO_2(1:8), and 1%Au/CeO_2 calcined at 400°C are shown in Figure 4.2. There is no evidence of gold metallic peaks in all catalysts, which means that the gold particle size could be less than 5 nm. Moreover, it can be seen that the diffraction of 1%Au/CeO_2 presents a very strong peak at $2\theta = 28.5°$, which is characteristics of fluorite structure of CeO_2. The other weak peaks at 33.08, 47.47, 56.33, 59.08, 69.40, 76.69, and 79.067 were corresponding to CeO_2 (200), CeO_2 (220), CeO_2 (311), CeO_2 (222), CeO_2 (400), CeO_2 (331), and CeO_2 (420) for $CuK\alpha$ (1.5406 Å) radiation, respectively. The XRD result does not change much when CeO_2 was mixed with a small amount of Fe_2O_3 as a support. However, from Figure 4.2, it can be seen that no Fe_2O_3 peaks characteristic appear in 1%Au/Fe_2O_3-CeO_2(1:8), which mean that Fe^{3+} has incorporated in the ceria lattice to form a solid solution (Lin *et al.*, 2008). Compared to the pure CeO_2 and the pure Fe_2O_3, the peaks of the CeO_2 and the Fe_2O_3, in the Fe_2O_3-CeO_2 composite catalysts become weaker. The reason is that the combination of Ce and Fe oxide in the catalyst can reduce the Fe_2O_3 and CeO_2 crystallite sizes (Sirichaiprasert *et al.*, 2006).

Table 4.1 Crystallite sizes of the 1%Au over different supports.

Catalysts	Crystallite size (nm)				
	CeO_2(111)	CeO_2(200)	CeO_2(220)	Au(111)	Au(200)
1%Au/CeO_2	10.17	11.46	9.16	<5	<5
1%Au/Fe_2O_3-CeO_2	10.36	11.36	7.95	<5	<5
1%Au/Fe_2O_3	-	-	-	<5	<5

From Table 4.1, it was found that the crystallinity of the CeO_2 of 1%Au/Fe$_2$O$_3$-CeO$_2$(1:8) slightly decreases when compared to 1%Au/CeO$_2$, which is in agreement with Sirichaiprasert *et al.*, 2006 and Hongyan *et al.*, 2008.
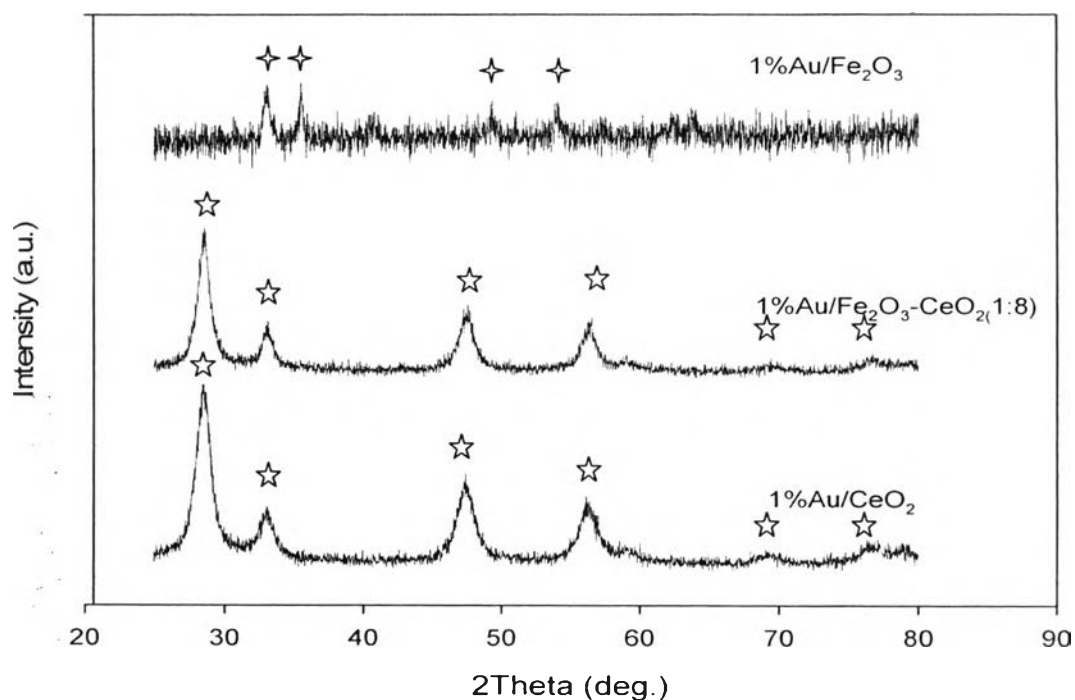

Figure 4.2 XRD patterns of supported Au catalysts ; (☆) CeO$_2$, (✦) Fe$_2$O$_3$

4.1.1.2 Surface Area Measurement (BET)

The surface areas of 1%Au/CeO$_2$, 1%Au/Fe$_2$O$_3$-CeO$_2$(1:8), and 1%Au/Fe$_2$O$_3$ are summarized in Table 4.2. The 1%Au/Fe$_2$O$_3$-CeO$_2$(1:8) had the highest surface area (142.2 m^2/g) than the pure Fe and Ce oxides. It can be observed that the combination of CeO$_2$ and Fe$_2$O$_3$ affects the surface area of the prepared catalyst which is in agreement with Honyan *et al.*, 2008. Consequently, the higher value of specific surface area of the Au/Fe$_2$O$_3$-CeO$_2$ catalysts was observed. It has been reported that by introducing different elements into the cubic lattice of a fluorite-structured material like CeO$_2$, the transport properties of the corresponding doped oxide are greatly affected as a result of the creation of

structural defects in the lattice (Leitenburg *et al.*, 1995). On the other hand, it has been reported that Ce^{4+} ions induce the creation of structural defects in the host metal oxide, leading to smaller grain size and a higher surface area (Sahoo *et al.*, 2009).

Table 4.2 BET surface areas of 1%Au/CeO$_2$, 1%Au/Fe$_2$O$_3$-CeO$_2$(1:8), and 1%Au/Fe$_2$O$_3$ catalysts

Catalyst	BET surface area (m^2/g)
1%Au/CeO$_2$	92.5
1%Au/Fe$_2$O$_3$-CeO$_2$(1:8)	142.2
1%Au/Fe$_2$O$_3$	85.5

4.1.1.3 Temperature-Programmed Reduction

The temperature-programmed reduction (TPR) technique was used to study the reduction profiles of the catalysts. Figure. 4.3 shows the TPR profiles of Au over different supports. For the Au/Fe$_2$O$_3$ catalyst, two reductions temperatures at 135°C and 320°C are found. The reduction peaks centered at 135°C is attributed to the reduction of Au$_x$O$_y$ species, present in the catalyst and the peak at 320°C is attributed to the reduction of Fe$_2$O$_3$ to Fe$_3$O$_4$ (Venugopal *et al.*, 2003). The high temperature reduction peak at 672°C is attributed to the reduction of Fe$_3$O$_4$ to FeO species (Venugopal *et al.*, 2003). The Au/CeO$_2$ shows the distinct peak at 139°C which has been reported as Ceria surface reduction peak when it is modified by incorporation of Au (Huang *et al.*, 2009). It clearly seen that the peak of the 1%Au/Fe$_2$O$_3$-CeO$_2$(1:8) at low temperature could occur from the combination of both the 1%Au/Fe$_2$O$_3$ and the 1%Au/CeO$_2$. The results indicated that there is a strong interaction between the Ce and Fe species, which agrees with the XRD results.
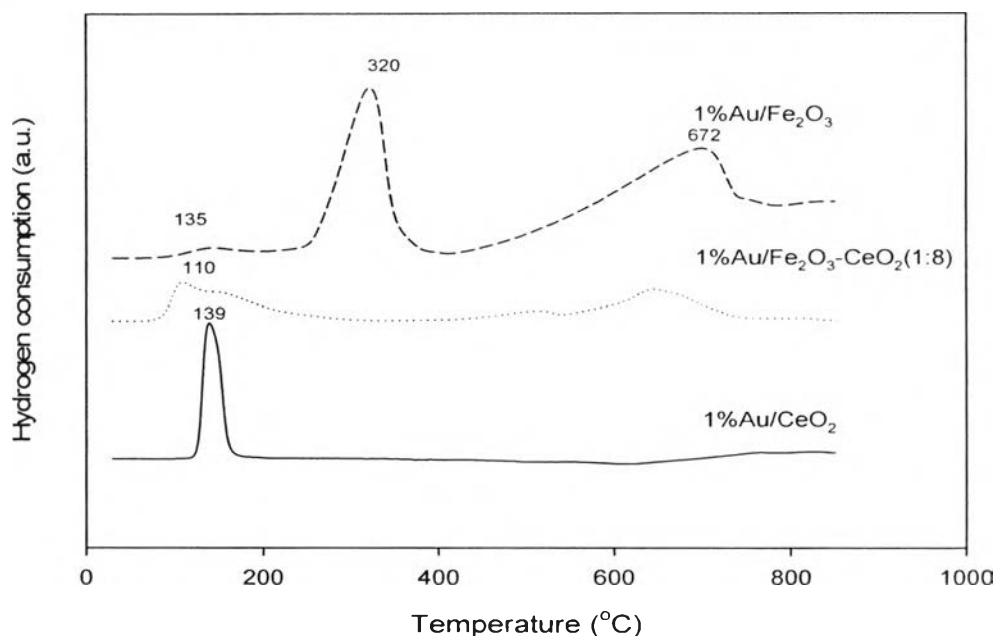
Figure 4.3 TPR profiles of 1%Au over different supports.

After this study, the combination of support between Fe_2O_3 and CeO_2 was selected to study more about the appropriate mole ratio between Fe_2O_3 and CeO_2.

4.1.2 Effect of Fe_2O_3-CeO_2 mole ratio on the catalytic performance

The combination of Fe_2O_3 and CeO_2 from previous section exhibited surprisingly results when compared to pure CeO_2 and Fe_2O_3. To study the influences of Fe_2O_3-CeO_2 mole ratio, the catalysts were prepared by deposition-precipitation technique with 1%Au content and various Fe_2O_3-CeO_2 mole ratios of 1:8, 1:1, 8:1. All catalysts were calcined at 400°C for 3 hours and tested in the methanol steam reforming reaction in the temperature range of 250 to 450°C.

From Figure 4.4, It can be seen that the 1%Au/Fe_2O_3-CeO_2(1:8) gave the highest methanol conversion and hydrogen selectivity of 93% and 73%, respectively. The catalytic performance of the iron-modified samples, 1%Au/Fe_2O_3-CeO_2(8:1) and 1%Au/Fe_2O_3-CeO_2(1:1), is very similar with the methanol conversion of 21% and 22%, and the H_2 selectivity of 67% and 65% at

350°C, respectively. The hydrogen selectivity of all catalysts remains constant in all range of the reaction temperature. From this result, it can be concluded that adding a small amount of Fe_2O_3 in CeO_2 will significantly improve the catalytic performance in the methanol steam reforming, which is supported by Hongyan $et\ al.$, (2008). They conducted the experiment of ethanol steam reforming by nonoscale $Ce_xFe_{1-x}O_2$ solid solution catalyst and they found that a small amount of Fe in Ce showed better activity and hydrogen selectivity than CeO_2 and Fe_2O_3.
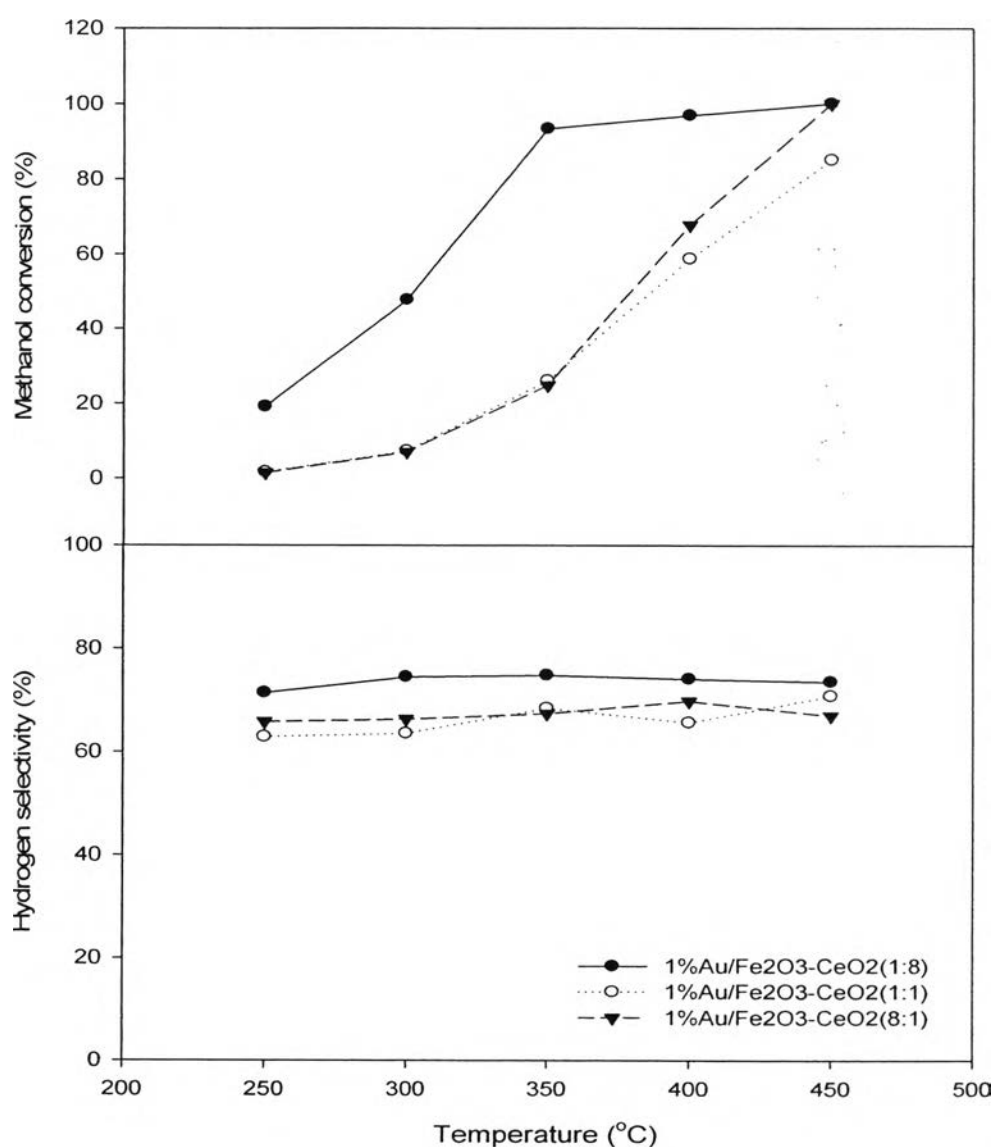
Figure 4.4 Effect of temperature on the methanol conversion and H_2 selectivity of supported Au catalysts

4.1.2.1 X-ray Diffraction (XRD)

Figure 4.5 shows the XRD patterns of supported Au catalysts prepared by deposition-precipitation, and calcined at 400°C. It was found that a hexagonal phase with hematite structure was observed for Fe_2O_3 support and a cubic phase with fluorite structure for CeO_2 support. The $1\%Au/Fe_2O_3$-$CeO_2(8:1)$ were amorphous and it can be seen very weak diffraction peaks of the hematite, whereas the characteristics of hematite could not be observed on the XRD patterns of $1\%Au/Fe_2O_3$-$CeO_2(1:1)$ and $1\%Au/Fe_2O_3$-$CeO_2(1:8)$ which is in agreement with Hongyan *et al.,* 2008 and Kongzhai *et al.,* 2008. In addition, the combination of CeO_2 and Fe_2O_3 in the catalysts could reduce the CeO_2 and Fe_2O_3 crystallite size. This result corresponds to the result of Hongyan *et al.,* 2008. Moreover, there is no evidence of a gold peak in all catalysts, implying that the gold particle size could be less than 5 nm.
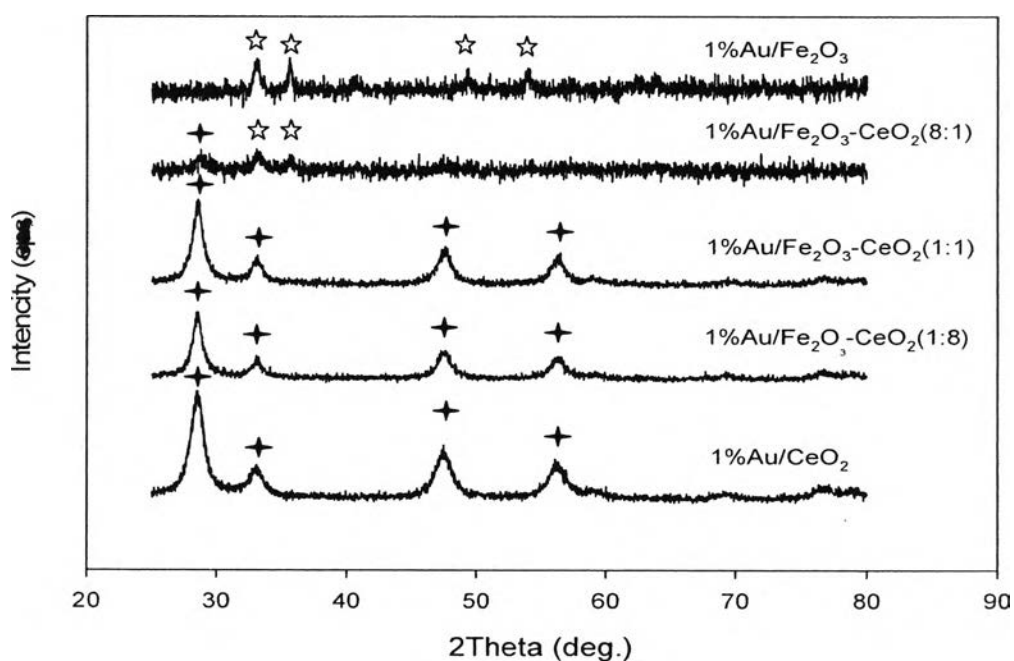
Figure 4.5 XRD patterns of 1%Au over different supports; (☆) Fe_2O_3, (+) CeO_2

Table 4.3 CeO$_2$ crystallite sizes of Au catalyst over different supports.

Catalysts	Crystallite sizes (nm)			Mean crystallite size (nm)
	CeO$_2$ (111)	CeO$_2$ (200)	CeO$_2$ (220)	
1%Au/CeO$_2$	10.17	11.45	9.16	10.26
1%Au/Fe$_2$O$_3$-CeO$_2$(1:8)	10.35	11.30	7.95	9.86
1%Au/Fe$_2$O$_3$-CeO$_2$(1:1)	8.93	18.16	20.33	15.80
1%Au/Fe$_2$O$_3$-CeO$_2$(8:1)	21.00	16.54	133.43	56.97

Table 4.3 shows the mean crystallite sizes of CeO$_2$ estimated by Scherrer equation in the 1%Au/CeO$_2$, 1%Au/Fe$_2$O$_3$-CeO$_2$(1:8), 1%Au/Fe$_2$O$_3$-CeO$_2$(1:1), and 1%Au/Fe$_2$O$_3$-CeO$_2$(8:1). The mean crystallite sizes of CeO$_2$ in the 1%Au/Fe$_2$O$_3$-CeO$_2$(1:8) was about 9.86 nm, whereas the mean crystallite sizes of CeO$_2$ in 1%Au/CeO$_2$, 1%Au/Fe$_2$O$_3$-CeO$_2$(1:1), and 1%Au/Fe$_2$O$_3$-CeO$_2$(8:1) were about 10.26, 15.80, and 56.97 nm, respectively.

4.1.2.2 Surface Area Measurement (BET)

The surface areas of the 1%Au/Fe$_2$O$_3$-CeO$_2$(1:8), 1%Au/Fe$_2$O$_3$-CeO$_2$(1:1), and 1%Au/Fe$_2$O$_3$-CeO$_2$(8:1) are summarized in Table 4.4. It is clearly seen that the addition of a small fraction of Fe into CeO$_2$ resulted in a remarkable increase in the surface area of the prepared catalysts.

Table 4.4 BET surface areas of 1%Au/Fe$_2$O$_3$-CeO$_2$(1:8), 1%Au/Fe$_2$O$_3$-CeO$_2$(1:1), and 1%Au/Fe$_2$O$_3$-CeO$_2$(8:1) catalysts

Catalyst	BET surface area (m^2/g)
1%Au/Fe$_2$O$_3$-CeO$_2$(1:8)	142.2
1%Au/Fe$_2$O$_3$-CeO$_2$(1:1)	117.4
1%Au/Fe$_2$O$_3$-CeO$_2$(8:1)	103.3

4.1.2.3 Temperature-Programmed Reduction

The temperature-programmed reduction (TPR) technique was applied to study the reduction profile of the catalysts. Figure 4.6 shows the TPR profiles of the CeO_2, Au/CeO_2, Au/Fe_2O_3, Au/Fe_2O_3-CeO_2 (1:8), Au/Fe_2O_3-CeO_2 (1:1), Au/Fe_2O_3-CeO_2 (1:8), Au/Fe_2O_3, and Fe_2O_3 catalysts. The bulk CeO_2 shows the center of reduction peak at 500°C (Huang *et al.*, 2009). It clearly seen that the incorporation of Au remarkably modifies the TPR profiles from 500°C to 139°C. This peak attributed to the reduction peak of the surface ceria, while the reduction peak of the ionic gold species can be neglected. Boccuzzi *et al.*, (1999) reported that metallic gold is analogy with other noble metals could activate the hydrogen with subsequent spillover on the support and promotion of the ceria reduction at lower temperature. It has also been suggested that the surface oxygen reducibility may enhanced through a lattice substitution effect, i.e., the vacant Ce^{4+} filled with the Au^+ of Au^{3+} would lead to the formation of oxygen vacancies and thus improve the oxygen mobility and reducibility (Fu *et al.*, 2003). For the bulk iron oxide showed two distinct reduction peaks with values of Tmax of 411 and 672°C. The first reduction peak at 411°C is attributed to the reduction of Fe_2O_3 to Fe_3O_4 was observed (Venugopal *et al.*, 2003). The high temperature reduction peak at 672°C is attributed to the reduction of Fe_3O_4 to FeO species (Venugopal *et al.*, 2003). For the Au/Fe_2O_3 catalyst, two reduction peaks at 135°C and 320°C are found. The reduction peaks centered at 135°C is attributed to the reduction of Au_xO_y species, present in the catalyst (Venugopal *et al.*, 2003). It is clearly seen from the TPR profiles of the Au/Fe_2O_3 catalyst that the low temperature reduction peak at 411°C is slightly decreased to 320°C, which indicates that Au exerts a positive influence on the ease of Fe_2O_3 reduction that occurs at lower temperatures. For the 1%Au/Fe_2O_3-CeO_2 catalysts, it is clearly seen that the peak at the temperature range of 100 to 400°C will split into two peaks with increasing the ratio of Fe. This result indicates that a small amount of Fe in the complex oxide will reduce the reduction temperature.
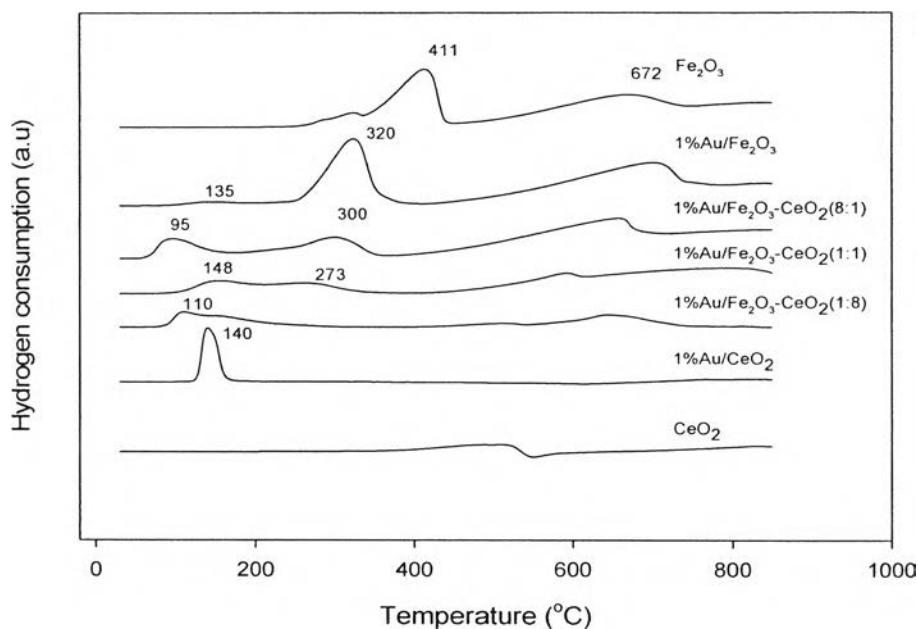
Figure 4.6 H$_2$-TPR profiles of the catalysts.

From this study, the 1%Au/Fe$_2$O$_3$-CeO$_2$(1:8) was selected to study further in next section.

4.1.3 Effect of Calcination Temperature on the Catalytic Performance

To study the effect of the calcination temperature on the activity of 1%Au/Fe$_2$O$_3$-CeO$_2$(1:8), the catalysts prepared by deposition-precipitation technique were annealed before the reaction at three different calcination temperatures of 300, 400, and 500°C for 3 hours. Activity tests were then conducted on each of the sample sets.

Figure 4.7 shows the effect of calcination temperature on the activity and selectivity of 1%Au/Fe$_2$O$_3$-CeO$_2$(1:8) catalysts. It is clearly seen that the calcination temperature significantly influenced the catalytic performance and hydrogen selectivity of the catalyst. Methanol conversion and hydrogen selectivity increased as the calcination temperature increased; however, when the calcination temperature up tills 500°C, its activity decreased. It can be concluded that the

appropriate calcination temperature was 400°C. The decreasing in activity was observed when the calcination temperature was higher than 400°C. The catalyst would undergo a little bit phenomenon of sintering. This effect can be attributed to the particles coarsening and TEM results in Figure 4.7 indicated that significant agglomoeration occurred in the sample calcined at 500°C.

From this study, the calcination temperature of 400°C was selected as the appropriate condition for the prepared catalysts.
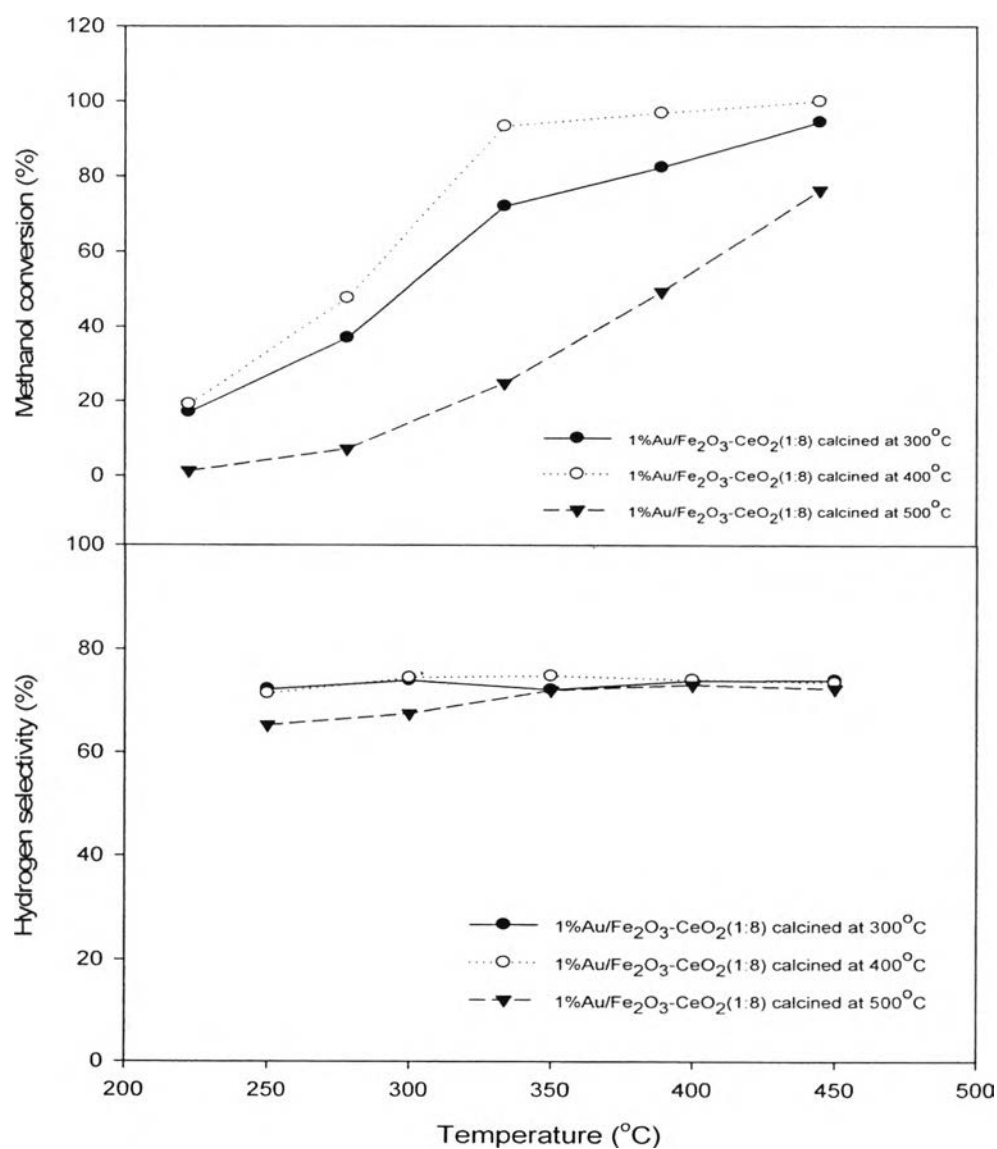
Figure 4.7 Effect of calcination temperature on the activity and selectivity of 1%Au/Fe$_2$O$_3$-CeO$_2$(1:8) catalyst.

4.1.3.1 Transmission Electron Micrograph (TEM)

Figure 4.8 shows the TEM images of the 1%Au/Fe$_2$O$_3$-CeO$_2$(1:8) with different calcination temperatures. The Au particles are seen as dark spot on the supports. The mean particle size of Au of Au/Fe$_2$O$_3$-CeO$_2$ with various calcinations temperatures of 300, 400, 500C were 3.16±0.78, 3.67±1.21, and 5.40±2.01 nm, respectively. The catalyst calcined at 500°C has the largest Au particle sizes compared to the catalysts calcined at 400°C and 300°C. This phenomena agrees with the activity testing. Therefore, it can be concluded that the suitable calcination temperature is 400°C.

50 nm
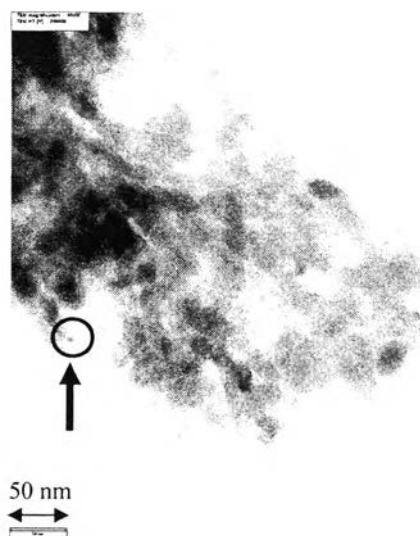
a) 1%Au/Fe$_2$O$_3$-CeO$_2$(1:8) calcined at 300°C
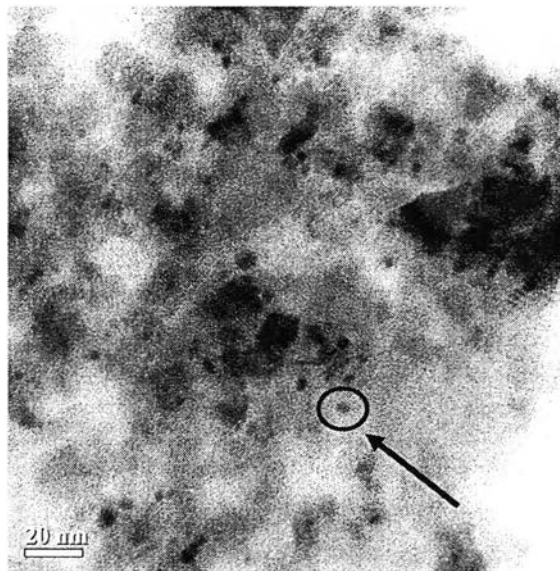
b) 1%Au/Fe$_2$O$_3$-CeO$_2$(1:8) calcined at 400°C
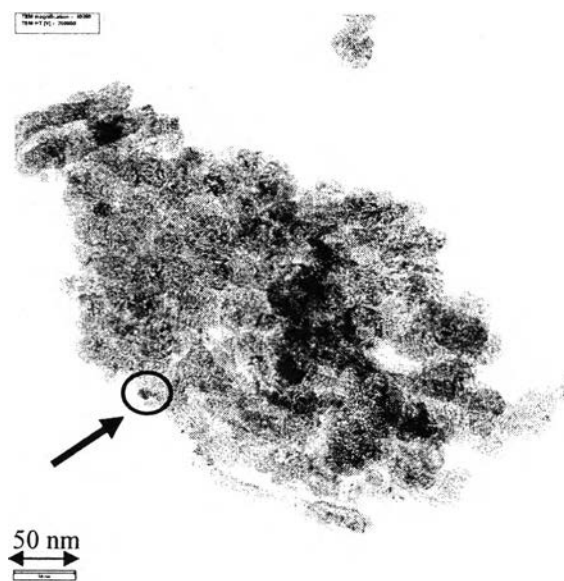
c) 1%Au/Fe$_2$O$_3$-CeO$_2$(1:8) calcined at 500°C
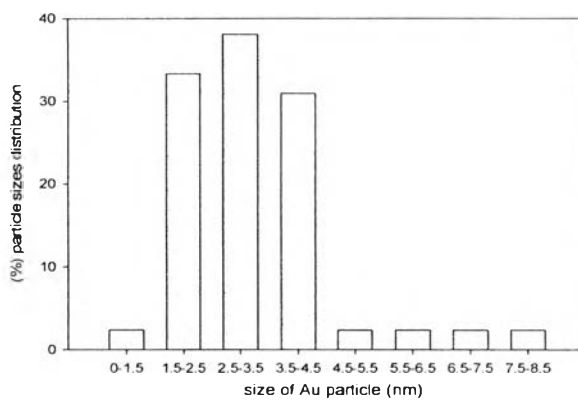
a) 1%Au/Fe$_2$O$_3$-CeO$_2$ calcinced at 300°C
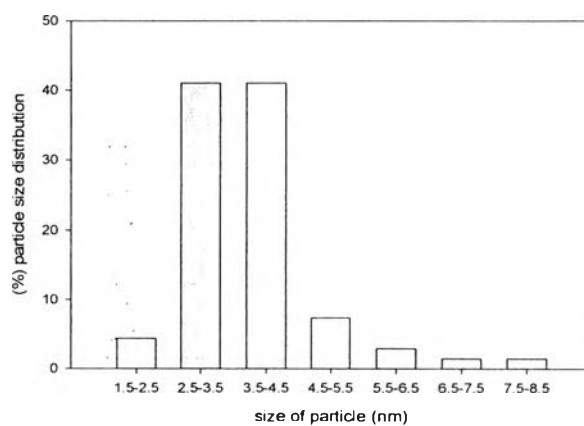
b) b) 1%Au/Fe$_2$O$_3$-CeO$_2$ calcinced at 400°C
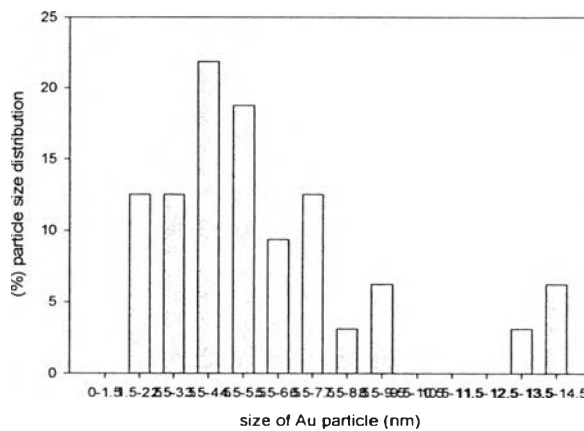
c) 1%Au/Fe$_2$O$_3$-CeO$_2$ calcinced at 500°C

Figure 4.8   TEM images and particle size distribution of 1%Au/Fe$_2$O$_3$-CeO$_2$(1:8) catalysts with various calcination temperatures.

4.1.4 Effect of Au content over Fe₂O₃-CeO₂(1:8) support

The Au/Fe$_2$O$_3$-CeO$_2$(1:8) catalysts were prepared by deposition-precipitation technique with various Au contents of 1%, 3% and 5% atom. All of these catalysts were calcined at 400°C for 3 hours.

The effect of Au content on Au/Fe$_2$O$_3$-CeO$_2$(1:8) catalysts on both methanol conversion and hydrogen selectivity is shown in Figure 4.9. It was found that with increasing Au content, methanol conversion and hydrogen selectivity are decreased. The 1%Au content exhibited the highest performance, when compared to 3% and 5%Au, respectively.
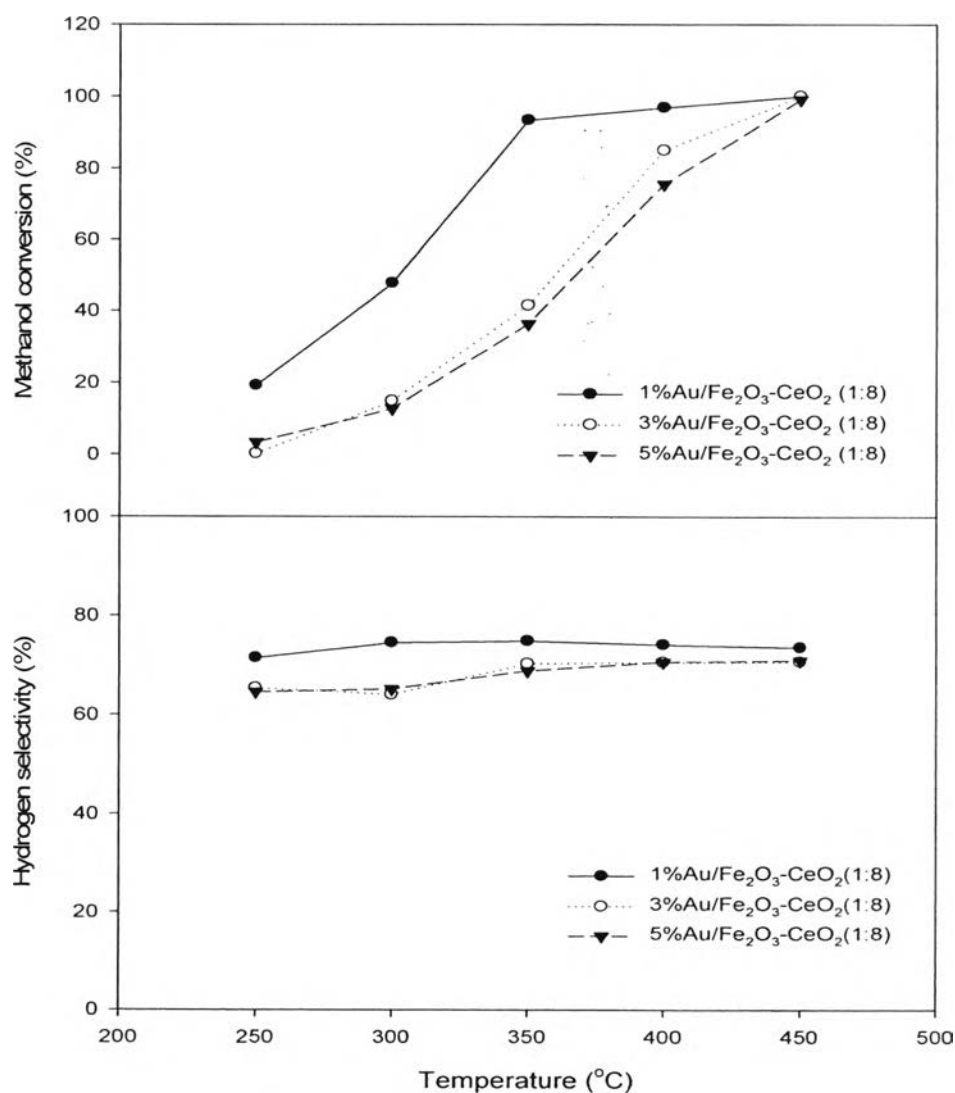
Figure 4.9 Effect of Au content on the activity and selectivity of the Au/Fe$_2$O$_3$-CeO$_2$(1:8) catalysts.

4.1.4.1 Transmission Electron Micrograph (TEM)

TEM micrographs of the Au/Fe_2O_3-CeO_2 catalyst with various Au contents are shown in Figure 4.10. The mean particle size of Au of Au/Fe_2O_3-CeO_2 with various Au contents of 1%, 3%, 5% atom were 3.67±0.05, 7.42±0.05. 7.69±0.05 nm, respectively. It was found that the particle size obviously increased with increasing Au content. In the activity testing, when increasing the Au content, the methanol conversion and hydrogen selectivity drop gradually. Therefore, it can be concluded that a large size of Au particle on the Au/Fe_2O_3-$CeO_2(1:8)$ was not preferred for the methanol steam reforming reaction.
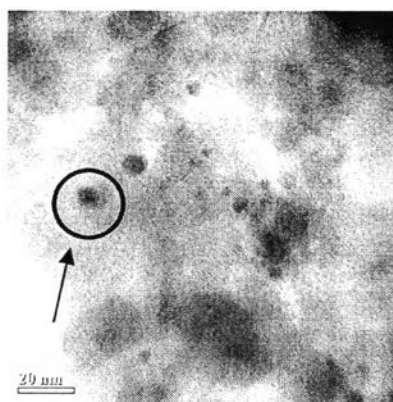
a) $1\%Au/Fe_2O_3$-$CeO_2(1:8)$
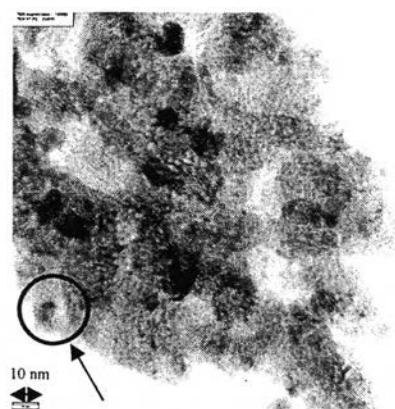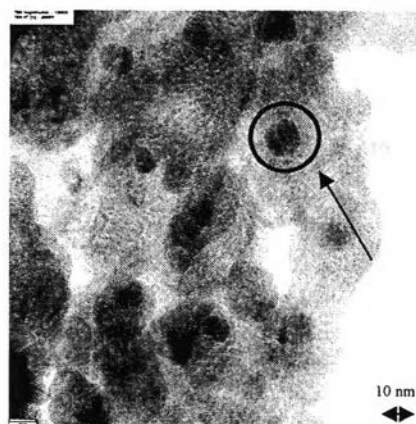
b) $3\%Au/Fe_2O_3$-$CeO_2(1:8)$
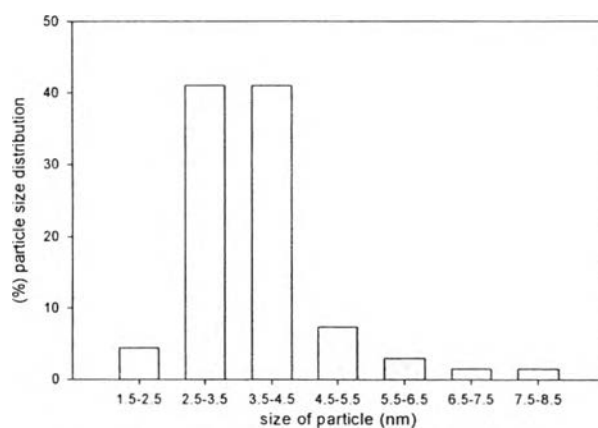
a) $5\%Au/Fe_2O_3$-$CeO_2(1:8)$

a) 1%Au/Fe$_2$O$_3$-CeO$_2$(1:8)
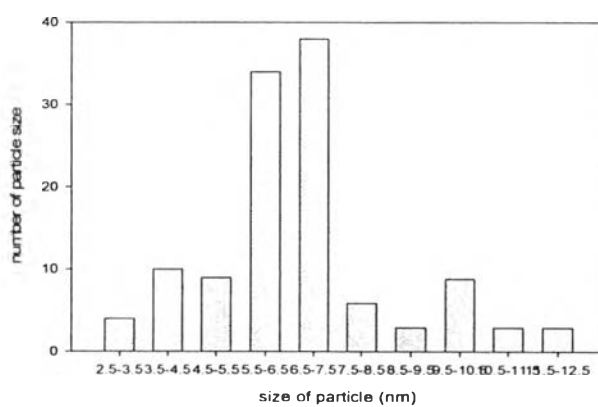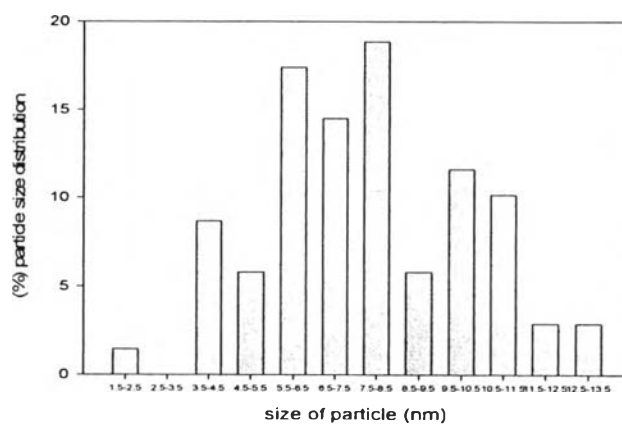
b) 3%Au/Fe$_2$O$_3$-CeO$_2$(1:8)

a) 5%Au/Fe$_2$O$_3$-CeO$_2$(1:8)

Figure 4.10 TEM images and particle sizes distribution of Au/Fe$_2$O$_3$-CeO$_2$(1:8) catalysts with various Au contents.

4.1.5 Effect of Catalyst Pretreatment

The pretreatment of catalyst is very important for chemical reaction. The different pretreatments will provide different characteristic of the catalysts. It is of interest to investigate the effect of pretreatments, which are H_2 reduction at 400°C and O_2 oxidation at 200°C for 1 hour on the activity and selectivity of 1%Au/Fe$_2$O$_3$-CeO$_2$(1:8) catalysts (calcined at 400°C). The effect of catalyst pretreatment on the activity and selectivity of 1%Au/Fe$_2$O$_3$-CeO$_2$(1:8) catalyst are shown in Figure 4.11. The activity of Au/Fe$_2$O$_3$-CeO$_2$ increased with an increase in reaction temperature and methanol conversion reached 100% at 450°C. However, the unpretreated catalyst exhibited higher activity than the catalyst pretreated with O_2 and H_2, respectively. The H_2 selectivity of all catalysts was more than 65% at the temperature range of 250 to 450°C. From XRD result, there is no any different peak. It could be suggest that the phase of support is not change when different pretreatment.
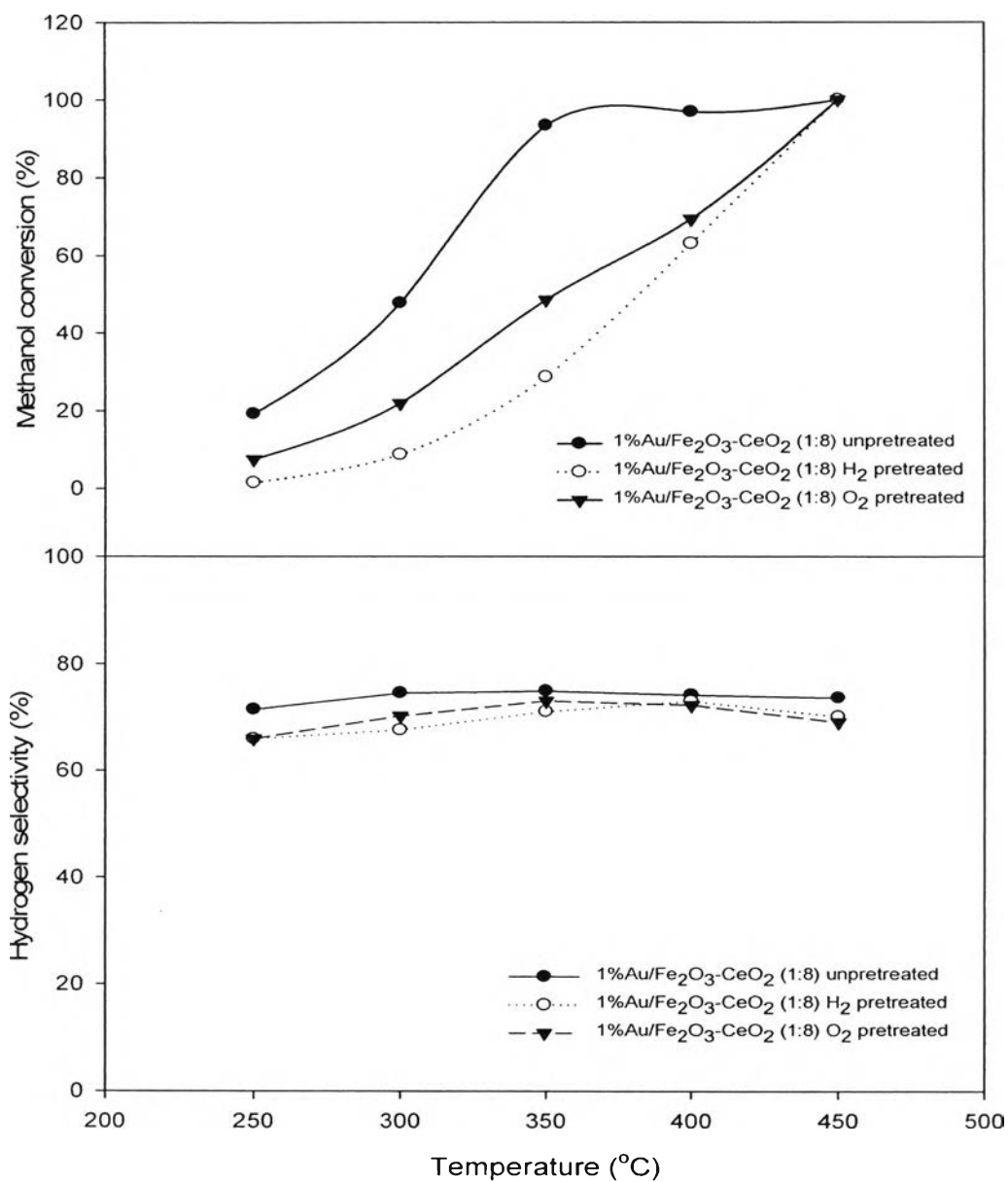
Figure 4.11 Effect of catalyst pretreatment on the activity and selectivity of the catalysts.

4.1.5.1 X-ray Diffraction (XRD)

Figure 4.12 shows the XRD patterns of the catalysts, which consisted of unpretreated, O_2 pretreated, and H_2 pretreated. There are no phase changing when catalyst are treated with different method. Implying that the gas pretreatment does not significantly affect the morphology of support.
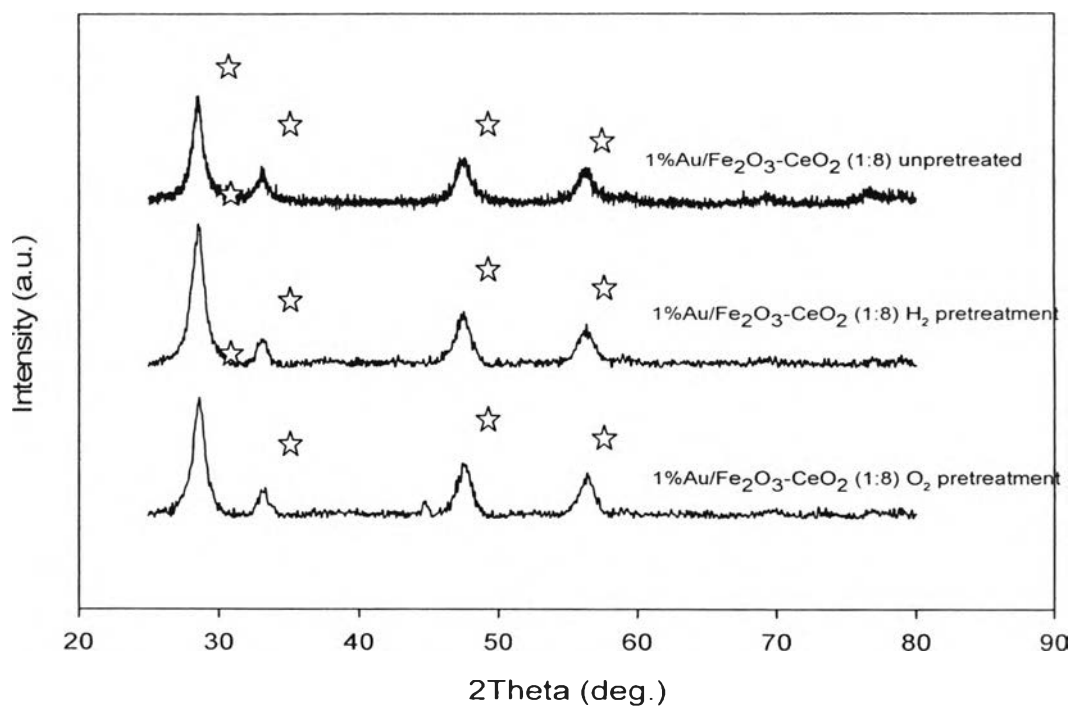
Figure 4.12 XRD patterns of the prepared catalysts; unpretreated, O_2 pretreatment, and H_2 pretreatment, (☆) CeO_2

4.1.6 Comparision of Acitivity and Selectivity between Support and Supported Au Catalysts

To study the catalytic behavior of the prepared catalysts, the catalytic activity of 1%Au/Fe_2O_3-CeO_2(1:8) and Fe_2O_3-CeO_2(1:8) catalysts were compared for the methanol steam reforming reaction at the temperature range of 250 to 450°C.
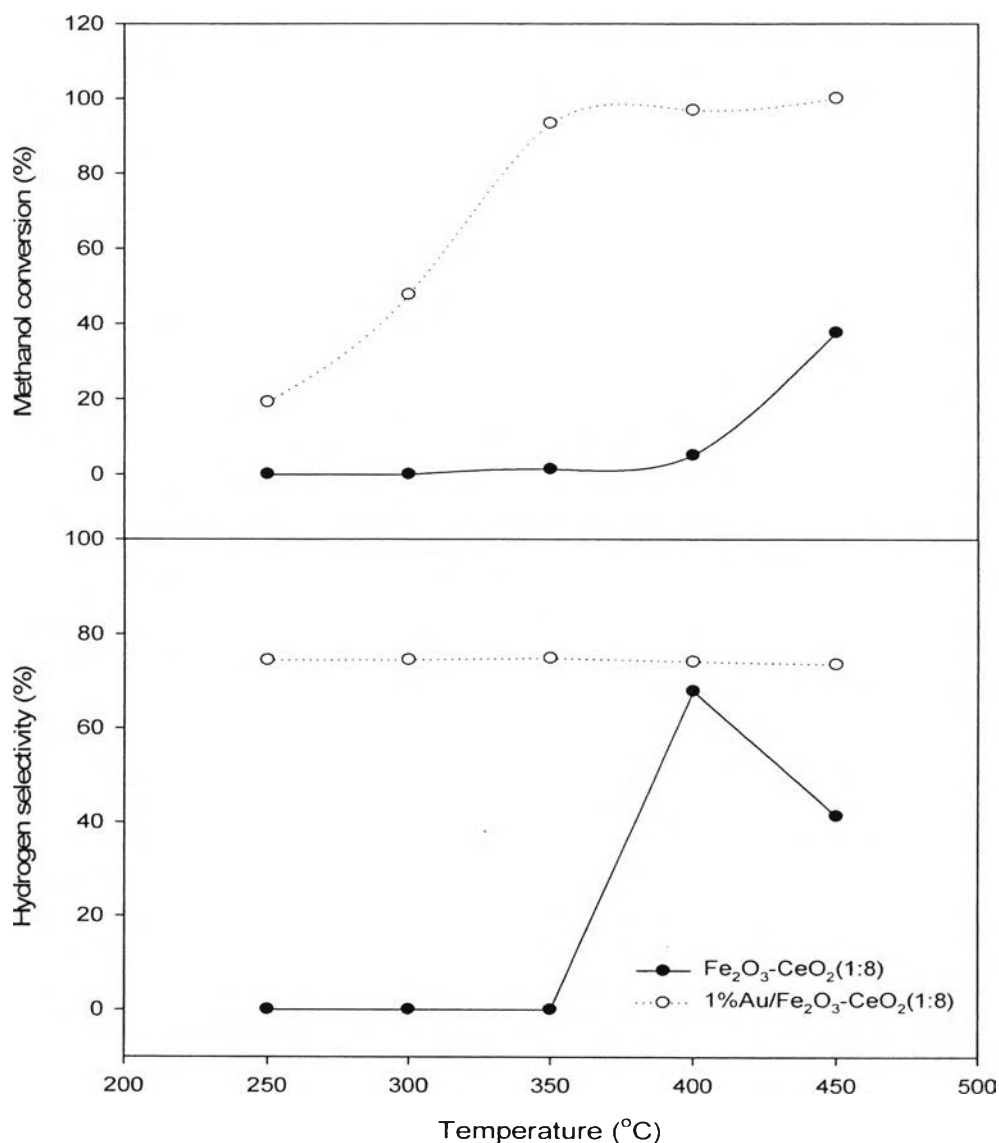
Figure 4.13 Catalytic activity of Fe_2O_3-CeO_2(1:8) and 1%Au/Fe_2O_3-CeO_2(1:8).

Figure 4.13 shows the methanol conversion and hydrogen selectivity of 1%Au/Fe_2O_3-CeO_2(1:8) and Fe_2O_3-CeO_2(1:8). It can be concluded that Au is the active site for the methanol steam reforming. For the support alone, the Fe_2O_3-CeO_2(1:8) does not show any activity at low temperatures (250–350°C); however, at temperature higher than 400°C support shows some activity and selectivity.
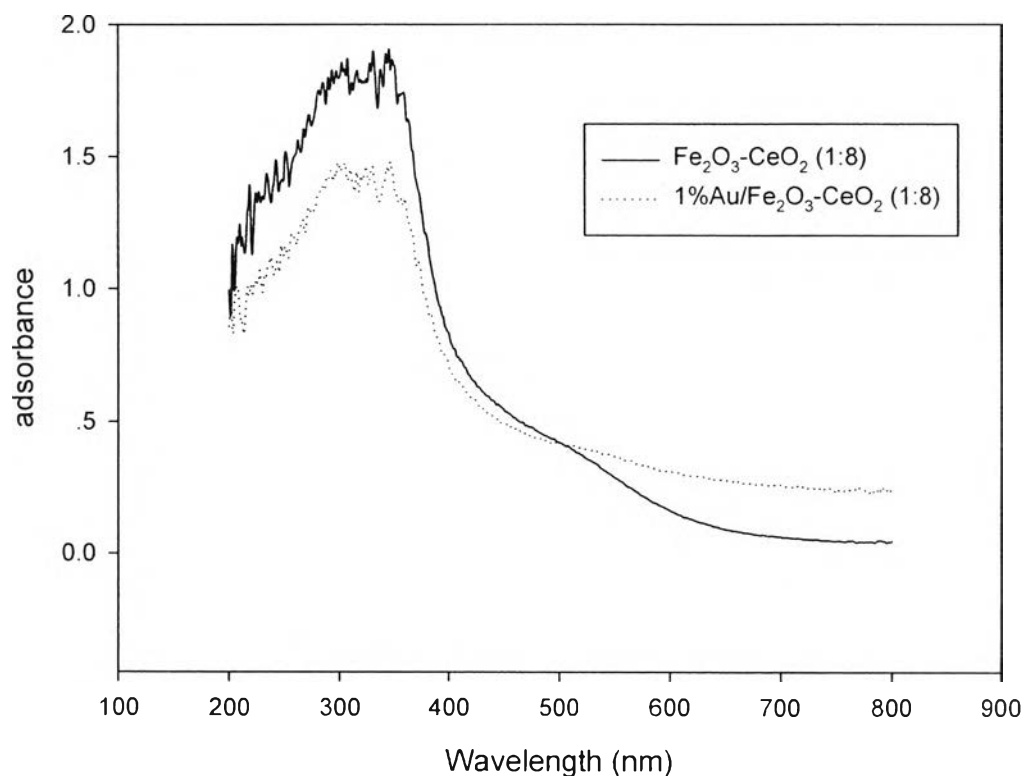
Figure. 4.14 UV-vis spectroscopy of $Fe_2O_3\text{-}CeO_2(1:8)$ and $1\%Au/Fe_2O_3\text{-}CeO_2(1:8)$.

    In recent years, there are many research works study the present of Au metal by using UV-vis spectroscopy to identify the substantive gold metal on support. The metallic gold peak, known to be located between 520-570 nm for gold particle on metal oxides (Guzman and Corma., 2005). In this present work, Figure 4.14 and 4.15 show the UV-vis spectroscopy result. Due to the interfering of combination of support and the Plasmon resonance band of Au metallic, so it cannot interpret to identify the substantive gold metal on support.
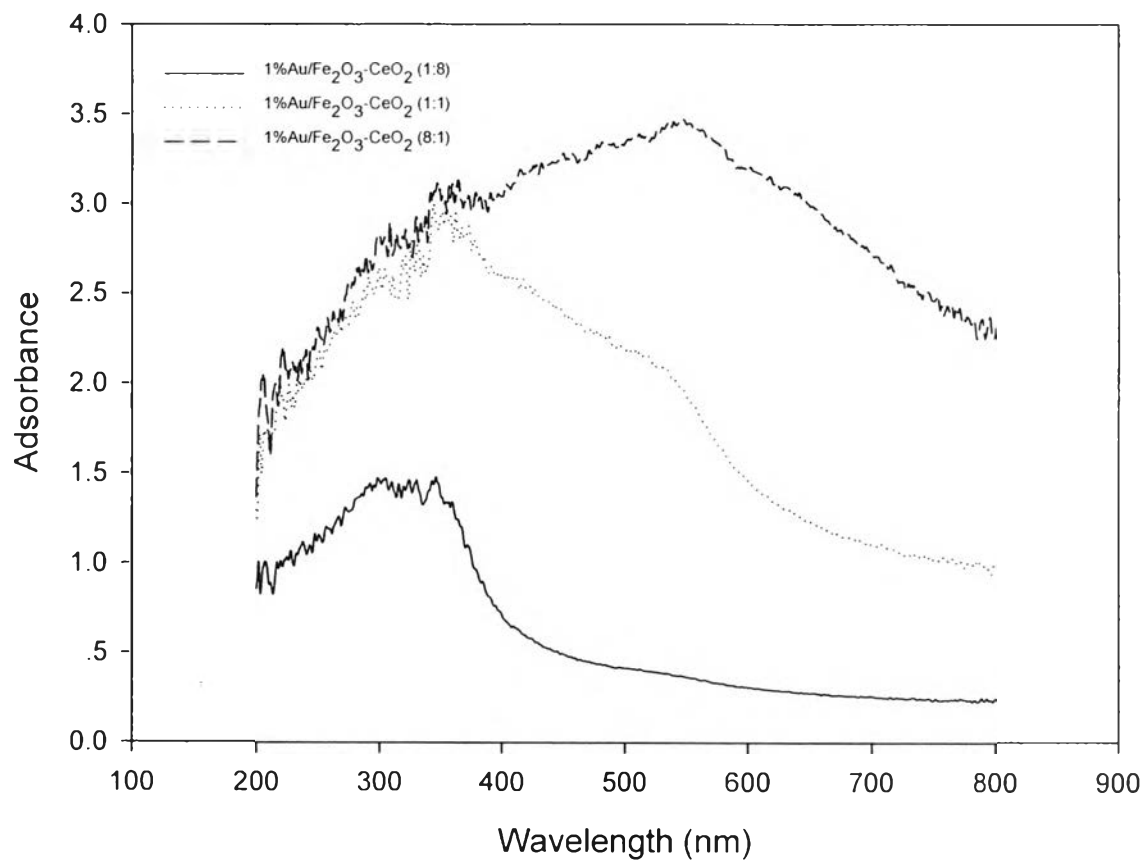
Figure 4.15 UV-vis spectroscopy of 1%Au/Fe$_2$O$_3$-CeO$_2$(1:8), 1%Au/Fe$_2$O$_3$-CeO$_2$(1:1), and 1%Au/Fe$_2$O$_3$-CeO$_2$(8:1).

4.2 Stability testing and Side reactions (WGS and DM)

From previous section, the 1%Au/Fe$_2$O$_3$-CeO$_2$(1:8) calcined at 400°C exhibited the best catalytic. In this part, the 1%Au/Fe$_2$O$_2$-CeO$_2$(1:8) was performed in the water gas shift and the decomposition of methanol reaction to study the catalytic performance in two side reactions. In addition, the stability of this catalyst was carried out.

4.2.1 Stability Testing

The catalytic stability of 1%Au/Fe$_2$O$_3$-CeO$_2$(1:8) catalyst calcined at 400°C for 3 hours, which showed the maximum methanol conversion and H$_2$ selectivity, was tested at the constant temperature of 400°C. Figure 4.14 shows the performance of methanol reforming over 1%Au/Fe$_2$O$_3$-CeO$_2$ for 24 hours of testing time. It can be seen the methanol conversion slightly decreased.
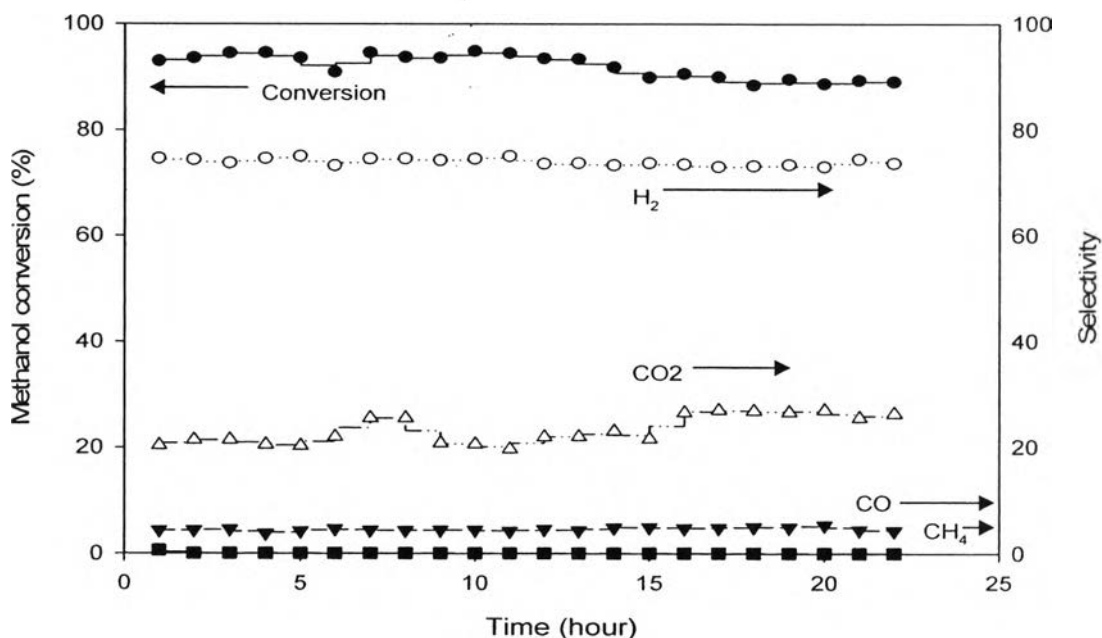

Figure 4.14 Stability testing of the 1%Au/Fe$_2$O$_3$-CeO$_2$(1:8) at 400°C for 24hours.

4.2.1.1 Temperature-Programmed Oxidation (TPO)

Temperature-programmed oxidation (TPO) experiments were investigated on the prepared catalyst in order to measure the amount of carbon deposition (coke formation) on the 1%Au/Fe$_2$O$_3$-CeO$_2$(1:8) catalyst after the reaction was carried out at 450°C for 24 hours. It was found that the amount of carbon deposition was 0.4 % weight. Therefore, the coke formation does not affect the catalytic activity of the catalyst.
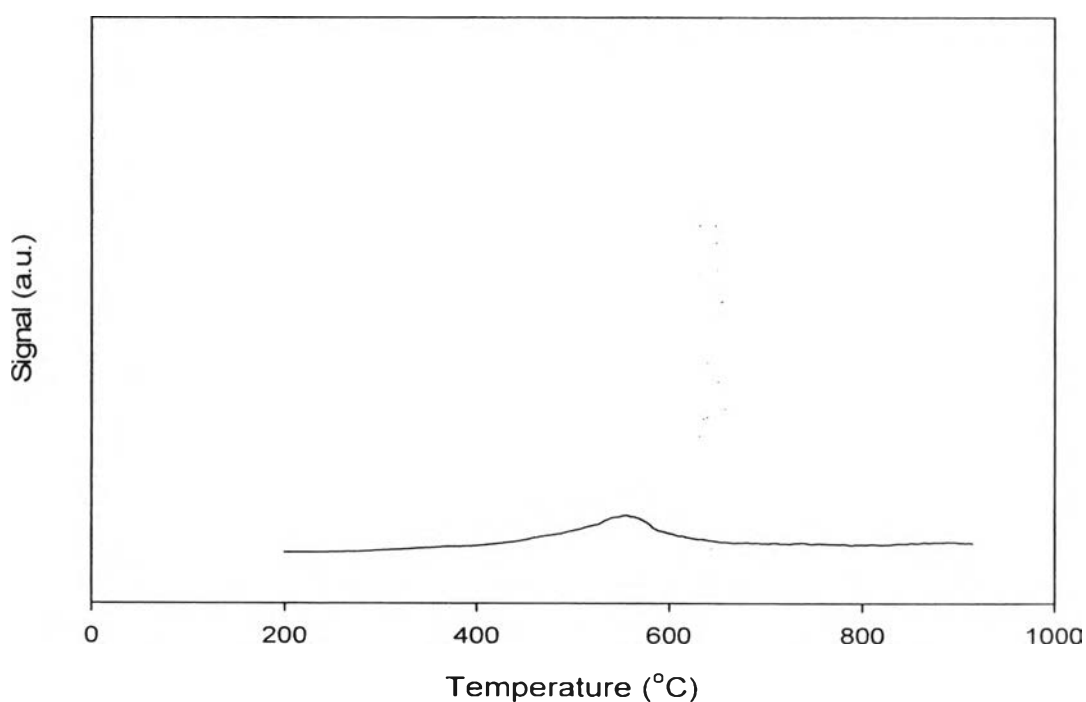

Figure 4.17 Temperature programmed oxidation profile of the 1%Au/Fe$_2$O$_3$-CeO$_2$(1:8).

4.2.2 Methanol Decomposition Reaction (DM)

In equation 4.1, the product of the methanol decomposition is hydrogen which is the main product from the methanol steam reforming. Methanol was decomposed mainly to CO and H$_2$ (equation 4.1) over this reaction. Therefore, it is necessary to study the 1%Au/Fe$_2$O$_3$-CeO$_2$(1:8) on the methanol decomposition reaction.

$$CH_3OH(g) \rightarrow 2H_2(g) + CO(g) \quad \Delta H^\circ_R = 128 \text{ kJmol}^{-1} \text{ (298 K)} \tag{4.1}$$
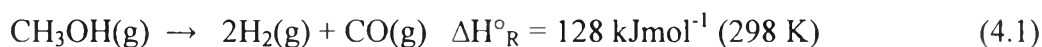
The reaction conditions were 1.5 ml/hour of liquid flow rate, 34 ml/min of carrier gas (He), and reaction temperature range of 250–450°C.

Figure 4.15 shows the catalytic activity in the decomposition of methanol reaction, it is clearly seen that the maximum methanol conversion of 55% was achieved at 450°C. The methanol conversion was very low, when operated at low temperature. It can be concluded that the 1%Au/Fe$_2$O$_3$-CeO$_2$(1:8) has better active for the steam reforming reaction than that in the decomposition of methanol reaction.

Figure 4.16 shows the product distribution of 1%Au/Fe$_2$O$_3$-CeO$_2$(1:8) in the decomposition of methanol reaction. Hydrogen selectivity of 60% remain constant in all range of temperature studied.
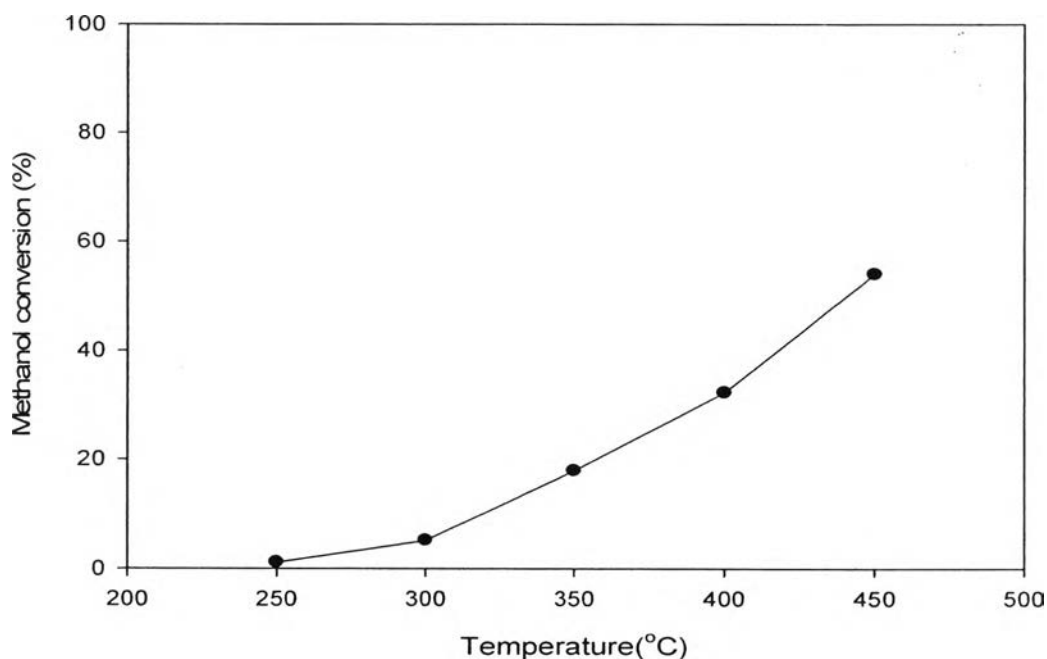

Figure 4.18 Catalytic performance of the 1%Au/Fe$_2$O$_3$-CeO$_2$(1:8) in the decomposition of methanol reaction.
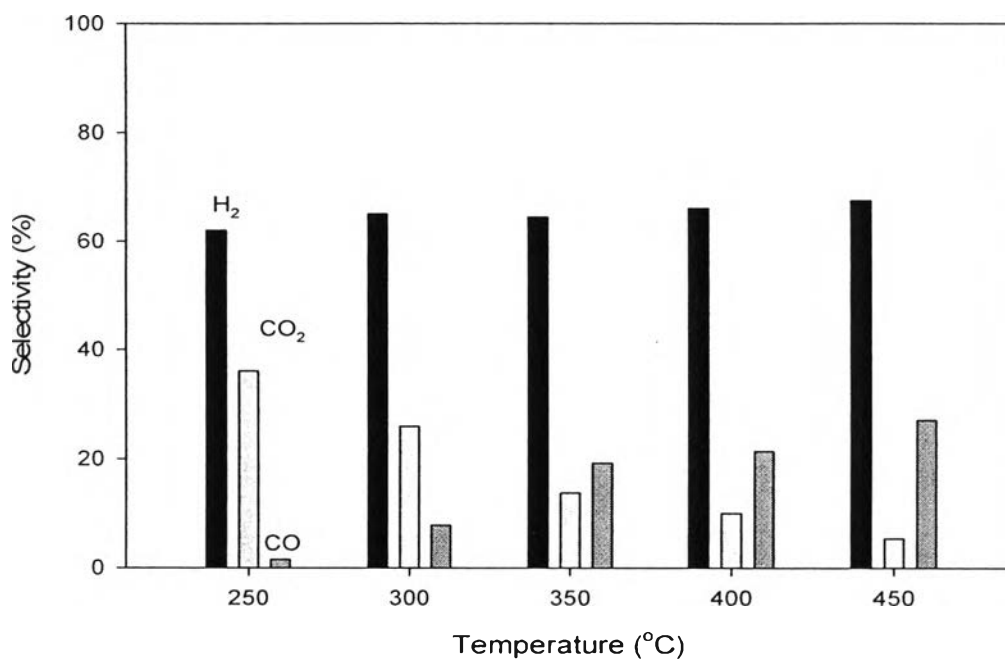
Figure 4.19 Product distribution of the decomposition of methanol reaction.

4.2.3 Water Gas Shift Reaction (WGS)

The water gas shift reaction (Equation 4.2) is one of the side reactions that occurred at the same time. It can convert CO from the decomposition of methanol reaction to CO_2. Therefore, it is necessary to study the activity of the $1\%Au/Fe_2O_3\text{-}CeO_2(1:8)$ catalyst in this reaction.

$$CO_{(g)} + H_2O_{(g)} \longleftrightarrow H_{2(g)} + CO_{2(g)} \quad \Delta H^\circ R = -41 \text{ kJmol}^{-1} \quad (4.2)$$

The reaction conditions were 1.5 ml/hours of liquid flow rate, a flow rate of at a 3:1 molar ratio of H_2O to CO, a flow of carrier gas (He) of 34 ml/min, and reaction temperature range of 250–450°C
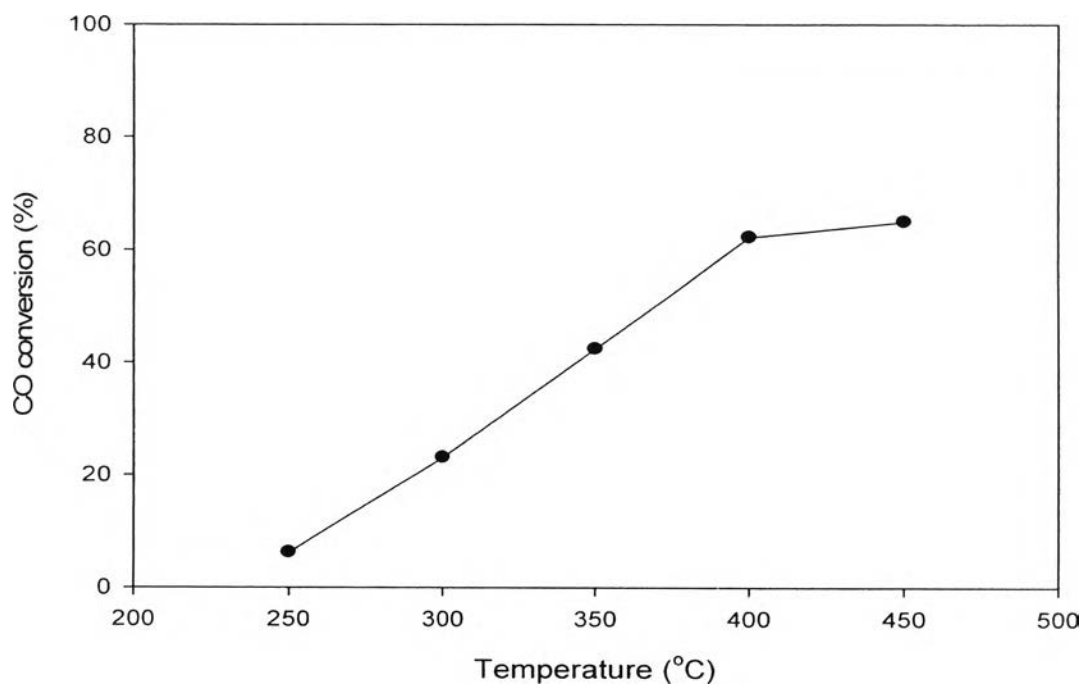
Figure 4.20 Catalytic activity of the 1%Au/Fe$_2$O$_3$-CeO$_2$(1:8) in water gas shift reaction.

From Figure 4.17, the CO conversion increased gradually when the temperature increase from 6.8% at 250°C to 65.3% at 450°C which means CO in product stream could occur from the decomposition of methanol reaction.